Infrared Spectra and Electronic Structure Calculations for the Group 2 Metal $M(OH)_2$ Dihydroxide Molecules

Xuefeng Wang and Lester Andrews*

Department of Chemistry, University of Virginia, P.O. Box 400319, Charlottesville, Virginia 22904-4319

Received: November 23, 2004; In Final Form: January 14, 2005

Reactions of laser-ablated Mg, Ca, Sr, and Ba atoms with O_2 and H_2 in excess argon give new absorptions in the O−H and O−M−O stretching regions, which increase together upon UV photolysis and are due to the $M(OH)_2$ molecules (M = Mg, Ca, Sr, and Ba). The same product absorptions are observed in the metal atom reactions with H_2O_2. The $M(OH)_2$ identifications are supported by isotopic substitution and theoretical calculations (B3LYP and MP2). The O−H stretching frequencies of the alkaline earth metal dihydroxide molecules decrease from 3829.8 to 3784.6 to 3760.6 to 3724.2 cm^{-1} in the family series in solid argon, while the base strength of the solid compounds increases. Calculations show that $Sr(OH)_2$ and $Ba(OH)_2$ are bent at the metal center, owing to d orbital involvement in the bonding. Although these molecules are predominantly ionic, the O−H stretching frequencies do not reach the ionic limit of gaseous OH^- going down the family group because of cation−anion polarization and $p_\pi \rightarrow d_\pi$ interactions.

Introduction

The group 2 metal dihydroxides are stable solids known for their increasing strength as bases with the heavier metals.[1] However, the isolated $M(OH)_2$ molecules have received little experimental investigation. The strongest infrared absorption of $Ca(OH)_2$ was observed upon irradiation of argon matrix samples containing Ca atoms and water.[2] The $Mg(OH)_2$ molecule was produced by laser-ablated Mg atom reactions where OMgO was thought to react with H_2 in excess argon.[3] The $Be(OH)_2$ species was observed in the reaction of laser-ablated Be atoms and water, and a C_2 structure with a linear OBeO linkage was computed for this molecule at the B3LYP level.[4] Further electronic structure calculations were done for the $M(OH)_2$ molecules at the MP2 level (M = Be, Mg, and Ca) and at the HF level (M = Ca, Sr, and Ba), but no vibrational frequencies were reported.[5,6] The Be species retains C_2 symmetry, the Mg and Ca dihydroxides favor linear structures, but the Sr and Ba dihydroxides are bent on the metal center based on these computations. Kaupp and Schleyer point out that these molecules are predominately ionic with a small covalency that acquires more d character going down the family group.[6]

More extensive electronic structure calculations have been done on the group 2 MOH molecules.[7−11] Trends in the bending potentials from the calculations and from experimental observations on the MgOH, CaOH, and SrOH molecules, for example,[12−18] suggested increased ionic character in this series. Recent observations add BaOH to this group.[19,20] This change also corresponds with a major increase in solubility of the solid $M(OH)_2$ compounds.[1] Finally, the $M(OH)_2$ molecules have not been observed in the gas phase, as even the MOH molecules require the MO + H_2 or M + H_2O reaction for mass spectrometer measurement of dissociation energies.[21] The M + H_2O_2 reaction has also been employed as a source of MOH molecules for high resolution laser spectroscopic investigations.[16]

Oxidative insertion reactions of Mg, Ca, Sr, and Ba atoms with water have been investigated in solid argon matrixes.[2] Upon photoexcitation of the metal atom, the major product was identified as the metal hydroxy hydride molecule HMOH. The use of water as a reagent in matrix-isolation investigations has some disadvantages: the O−H stretching region often masks important product absorptions, and contamination with natural isotopic water impurity in the system prevents pure isotopic substitution. We have discovered that reactions of metal atoms with mixtures of O_2 and H_2 provide some but not all of the same products as water without the above disadvantages. These reactions first form the OMO molecule which inserts into H_2 to produce the $M(OH)_2$ molecule. We also synthesize $M(OH)_2$ by the metal atom reaction with H_2O_2. Here, we report matrix infrared experiments and electronic structure calculations for the group 2 metal dihydroxide molecules. We observe a decrease in O−H stretching frequency in the series, which parallels an increase in ionic character. A preliminary communication on this work has appeared.[22]

Experimental and Computational Methods

Laser-ablated Mg, Ca, Sr, and Ba atom reactions with O_2 and H_2 in excess neon and hydrogen during condensation at 4 K and in argon at 8 K were performed as described in detail previously.[23] Isotopically enriched reagents (99% $^{18}O_2$, $^{16,18}O_2$-(20% $^{16}O_2$ + 50% $^{16}O^{18}O$ + 30% $^{18}O_2$), Yeda, and HD, D_2, Cambridge) were also employed. The Nd:YAG laser fundamental (1064 nm, 10 Hz repetition rate with 10 ns pulse width) was focused onto a rotating metal target (Johnson Matthey). Fresh metal targets were cut, filed clean, washed with dry hexane (Ca, Sr, and Ba), and placed in the vacuum chamber. The ablation laser energy was maintained as low as possible to avoid forming metal clusters in the matrix samples (typical energy is ∼1−3 mJ/pulse for neon experiments and ∼5 mJ/pulse for argon experiments). FTIR spectra were recorded at 0.5 cm^{-1} resolution on a Nicolet 750 instrument with 0.1 cm^{-1} accuracy using a liquid-nitrogen-cooled HgCdTe detector. Matrix samples were annealed at different temperatures and irradiated by a medium pressure mercury arc lamp (Philips, 175 W, globe removed) using optical filters for 20 min periods.

* Corresponding author. E-mail: lsa@virginia.edu.

10.1021/jp044660s CCC: $30.25
Published on Web 03/05/2005

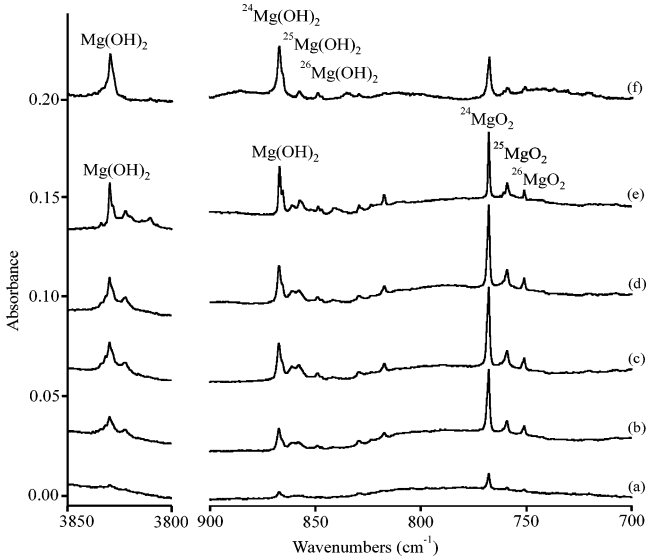

Figure 1. Infrared spectra in the 3850−3800 and 900−700 cm^{-1} regions for Mg, 0.4% O_2, 6% H_2, argon samples at 10 K: laser-ablated Mg (a) deposited for 60 min, (b) after 240−380 nm irradiation, (c) after $\lambda > 220$ nm irradiation, (d) after annealing to 10 K, and (e) after annealing to 20 K and (f) laser-ablated Mg deposited for 30 min with argon flowing over urea−hydrogen peroxide at room temperature and after $\lambda > 220$ nm irradiation.

Complementary density functional theory (DFT) calculations were performed using the Gaussian 98 program,[24] the B3LYP density functional, and the 6-311++G(3df,3pd) all-electron basis for H, Mg, and Ca and the SDD effective core potential and basis for Sr and Ba where 10 metal electrons were treated explicitly. Additional MP2 calculations were done for comparison.

Results

Infrared spectra from group 2 metal atom reactions with O_2, H_2 in excess argon and neon and electronic structure calculations on the metal dihydroxide molecules will be presented. These experiments gave the metal oxide and hydride product absorptions observed in previous investigations of each system separately[3,25−28] and absorptions for the HO_2 free radical.[29]

Mg. Infrared spectra of the $Mg/O_2/H_2$ system in excess argon are presented in Figure 1. Weak new bands appeared at 3829.8 and 867.2 cm^{-1} upon codeposition of laser-ablated Mg atoms with 0.4% O_2 and 6% H_2 in argon at 10 K along with MgH_2 (1571.8, 440.3 cm^{-1}) and OMgO (767.7 cm^{-1}).[3,25] Irradiation (240−380 nm) increased these bands 5-fold, and $\lambda > 220$ nm irradiation increased MgH_2 and OMgO by 25% and almost doubled the former new absorptions. Annealing to 15 K and further $\lambda > 220$ nm irradiation had no effect on the spectra. However, annealing to 20 K sharpened the product absorptions. The sharp 759.0 and 750.9 cm^{-1} satellites on the sharp 767.7 cm^{-1} $O^{24}MgO$ band are due to $O^{25}MgO$ and $O^{26}MgO$ in natural abundance.[25] Similar magnesium isotopic satellites at 857.4 and 848.6 cm^{-1} are observed on the major band shifted to 866.8 cm^{-1}. Infrared spectra of the Mg reaction products are compared with those found for Ca, Sr, and Ba in Figure 2.

Complementary experiments were done using argon flowing over urea−hydrogen peroxide (UHP), which has been employed as a source of H_2O_2 for matrix-isolation investigations.[30] Strong H_2O_2 absorptions were observed in solid argon at 3587.8 and 1270.8 cm^{-1} from the UHP reagent in a Teflon-valved Pyrex tube at room temperature along with weak water bands. The

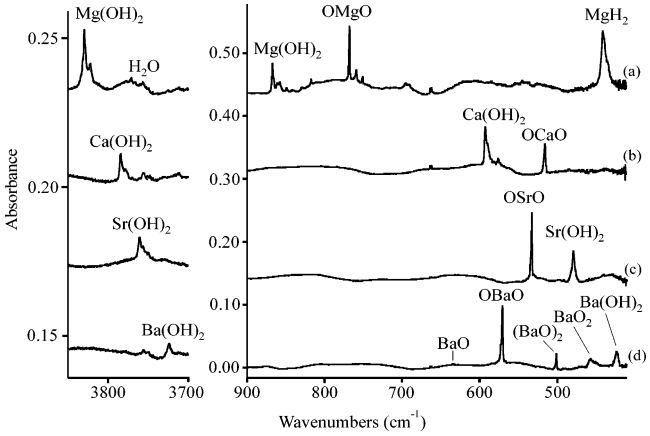

Figure 2. Infrared spectra in the 3850−3700 and 900−410 cm^{-1} regions for ultraviolet photochemical reaction products of Mg, Ca, Sr, and Ba atoms with 0.4% O_2 and 6% H_2 in solid argon at 10 K: (a) Mg; (b) Ca; (c) Sr; (d) Ba.

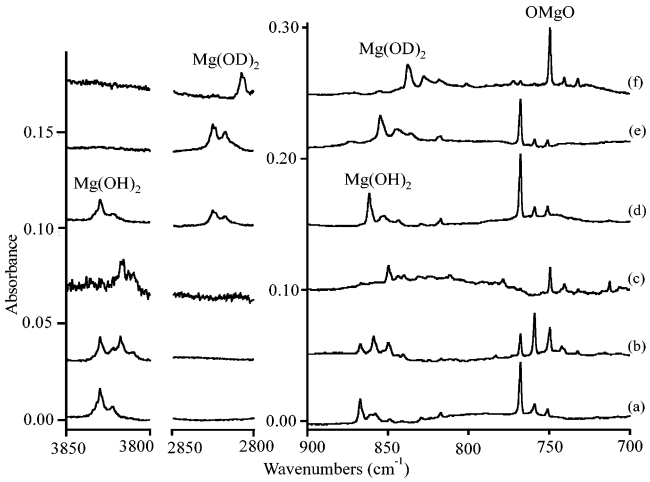

Figure 3. Infrared spectra in the 3850−3800, 2850−2800, and 900−700 cm^{-1} regions for Mg, 0.4% O_2, 6% H_2, argon samples at 10 K after 240−380 nm irradiation: (a) $^{16}O_2 + H_2$; (b) $^{16,18}O_2 + H_2$; (c) $^{18}O_2 + H_2$; (d) $^{16}O_2 + HD$; (e) $^{16}O_2 + D_2$; (f) $^{18}O_2 + D_2$.

major Mg atom reaction products were observed at 3829.7 and 866.9 cm^{-1}, almost the same as with the O_2 and H_2 reagents. These bands increased 10% upon 240−380 nm irradiation and 40% more upon $\lambda > 220$ nm irradiation, which gave sharper and cleaner product bands and more clearly resolved magnesium isotopic splittings for the 866.9 cm^{-1} band at 857.3 and 848.6 cm^{-1} than with $O_2 + H_2$. The latter spectrum is shown in Figure 1f for comparison. The OMgO absorption was also observed at 767.7 cm^{-1}. Another experiment with ice around the sample tube gave much reduced H_2O_2 absorption intensities, but the same two 3829.7 and 866.9 cm^{-1} product bands were observed with 25% of the total intensity. These experiments also produced bands at 3730 and 3633 cm^{-1} for the HOH···O complex identified previously.[30b]

Isotopically enriched O_2 and H_2 reagents were employed for the Mg reaction, and spectra are shown in Figure 3 after $\lambda > 220$ nm irradiation to maximize the new product absorptions, which are listed in Table 1. The 3829.8 cm^{-1} band became a 3829.8−3817.7 cm^{-1} doublet, and the 867.2 cm^{-1} band became a 867.2−858.9−850.0 cm^{-1} triplet with the $^{16,18}O_2$ (20% $^{16}O_2$, 50% $^{16}O^{18}O$, 30% $^{18}O_2$) sample. Using HD, the 3829.8 cm^{-1} band formed a 3829.8−2825.5 cm^{-1} doublet, but the 867.2 cm^{-1} band gave a single new band at 861.6 cm^{-1}. With D_2 and $^{16}O_2$, new bands appeared at 2825.5 and 854.8 cm^{-1}.[31]

TABLE 1: Infrared Absorptions (cm^{-1}) Produced upon Ultraviolet Irradiation of $Mg/O_2/H_2$ Samples in Solid Argon and Hydrogen

$^{16}O_2$, H_2	$^{16,18}O_2 + H_2$	$^{18}O_2 + H_2$	$^{16}O_2 + HD$	$^{16}O_2 + D_2$	$^{18}O_2 + D_2$
3829.8	3829.7, 3817.6	3817.7	3829.8, 2825.5	2825.5	2807.5
867.2[a]	867.2, 858.9, 850.0	850.0[b]	861.6[c]	854.8[d]	837.8[e]
3815.4[f]				2814.4[g]	
846.5				827.0	

[a] Band for ^{24}Mg product: ^{25}Mg and ^{26}Mg counterparts shifted 9.4 and 18.2 cm^{-1}. [b] Band for ^{24}Mg product: ^{25}Mg and ^{26}Mg counterparts shifted 9.5 and 18.6 cm^{-1}. [c] Band for ^{24}Mg product: ^{25}Mg and ^{26}Mg counterparts shifted 9.5 and 18.3 cm^{-1}. [d] Band for ^{24}Mg product: ^{25}Mg and ^{26}Mg counterparts shifted 9.9 and 19.0 cm^{-1}. [e] Band for ^{24}Mg product: ^{25}Mg and ^{26}Mg counterparts shifted 10.1 and 19.6 cm^{-1}. [f] Solid hydrogen. [g] Solid deuterium.

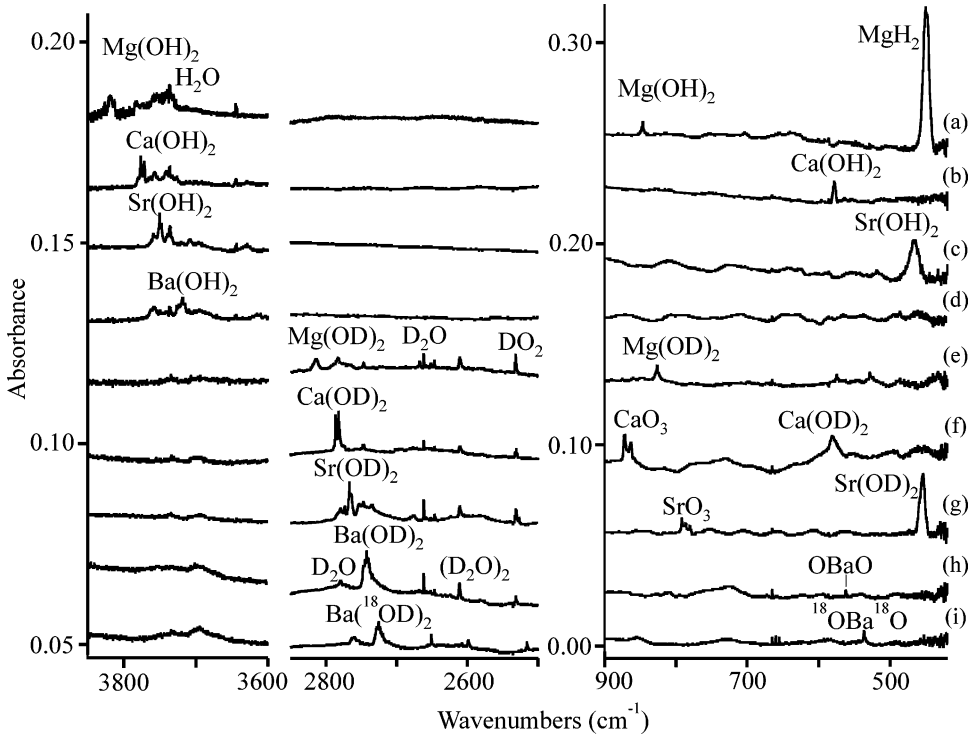

Figure 4. Infrared spectra in the 3850−3600, 2850−2500, and 900−420 cm^{-1} regions for ultraviolet photochemical reaction products of Mg, Ca, Sr, and Ba atoms with 0.2% O_2 in solid H_2 or D_2 at 4 K: (a) Mg; (b) Ca; (c) Sr; (d) Ba with $^{16}O_2$ in H_2; (e) Mg; (f) Ca; (g) Sr; (h) Ba with $^{16}O_2$ in D_2; (i) Ba with $^{18}O_2$ in D_2.

Similar experiments were performed using excess H_2 or D_2 with 0.1% O_2 as reagents. The new product bands shifted to 3815.4 and 846.5 cm^{-1} or to 2814.4 and 827.0 cm^{-1}, respectively. Figure 4 compares hydrogen and deuterium matrix spectra for the group 2 metal reactions.

Ca. Infrared spectra are shown in Figure 5 for laser-ablated Ca with O_2 and H_2. New absorptions are observed at 3784.6, 592.4, and 575.7 cm^{-1} in addition to weak CaO absorption at 746.7 cm^{-1}, sharp $(CaO)_2$ bands at 584.6, 516.5 cm^{-1} and OCaO at 515.6 cm^{-1},[26] and CaH_2 at 1216.3 cm^{-1}.[28] A weak 1232.3 cm^{-1} absorption is also observed, which along with the 575.7 cm^{-1} absorption, is due to HCaOH.[2] The latter bands increase little upon $\lambda > 290$ nm irradiation, but the 3784.6, 592.4, and 516.5 cm^{-1} bands increase markedly as does CaH_2. A subsequent 240−380 nm irradiation increases the 3784.6 and 592.4 cm^{-1} bands another 30% but slightly decreases the 516.5 cm^{-1} absorption.

An experiment was performed for the analogous Ca and H_2O_2 reaction, and two major new absorptions were observed at 3784.6 and 592.4, the same as using $O_2 + H_2$, with weaker bands at 1233, 746.7, 582.2, 575.7, 516.5, and 515.6 cm^{-1}. Full arc irradiation almost doubled the major product absorptions, while the H_2O_2 bands at 3587.8 and 1270.8 cm^{-1} decreased 30% and the H_2O absorptions and HOH···O complex absorptions increased. Figure 5 also compares spectra from the Ca and H_2O_2 reaction.

Figure 6 illustrates the spectra for isotopic O_2 and H_2 reagent substitution. With the $^{16,18}O_2$ sample, the upper band became a doublet and the 592.4 cm^{-1} band gave a triplet with an intermediate component at 585.1 cm^{-1} and an $^{18}O_2$ component at 575.3 cm^{-1}. The 575.7 cm^{-1} band was masked, but the intermediate region was clean, and the $HCa^{18}OH$ counterpart was observed at 556.6 cm^{-1}, near that reported by Kauffman et al.[2] Using $^{16}O_2$ and D_2 red shifted the upper band to 2792.0 cm^{-1}, as expected, but blue shifted the lower band to 594.8 cm^{-1}, an unusual deuterium shift. However, the HD reagent gave intermediate bands for both $^{16}O_2$ and $^{18}O_2$ at 593.6 and 578.6 cm^{-1} and doublets in the upper region. For the D_2 reagent, 240−380 nm irradiation also produced weak 1176 and 1168 cm^{-1} absorptions for D_2O and $D_2{}^{18}O$.[33]

Analogous investigations in excess neon with 3% H_2 and 0.2% O_2 gave broader 3782 cm^{-1} and sharper 606.7 cm^{-1} product absorptions, which increased upon UV irradiation, as footnoted in Table 2. Annealing decreased these absorptions and increased the 3730 and 586.2 cm^{-1} features. Neon matrix counterparts for other oxygen species[32] and Ca/O_2 products were also observed at 1164.6 and 973.1 cm^{-1} and at 795.6, 787.0, 646.6, and 636.7 cm^{-1}. With D_2 and $^{16}O_2$, new bands were

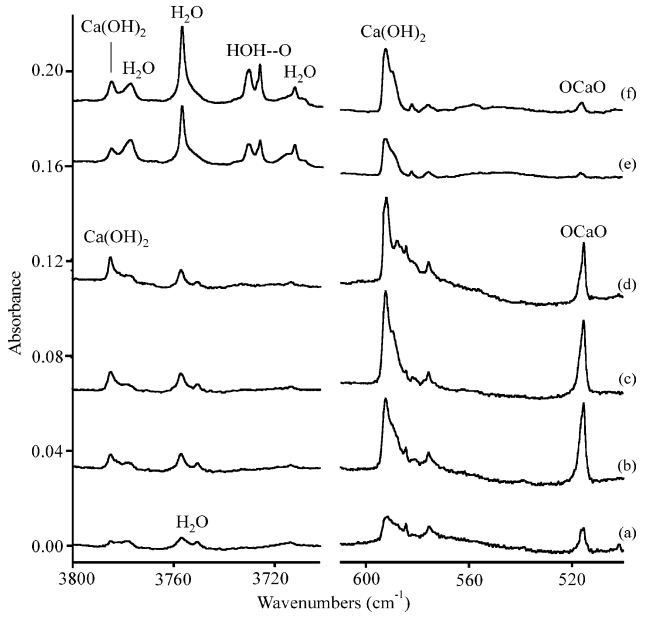

Figure 5. Infrared spectra in the 3800−3720 and 610−500 cm^{-1} regions for Ca atoms with 0.4% O_2 and 6% H_2 argon samples at 10 K: (a) laser-ablated Ca deposited, (b) after $\lambda > 290$ nm irradiation, (c) after 240−380 nm irradiation, and (d) after annealing to 20 K and (e) laser-ablated Ca deposited with argon containing H_2O_2 for 30 min and (f) after $\lambda > 220$ nm irradiation.

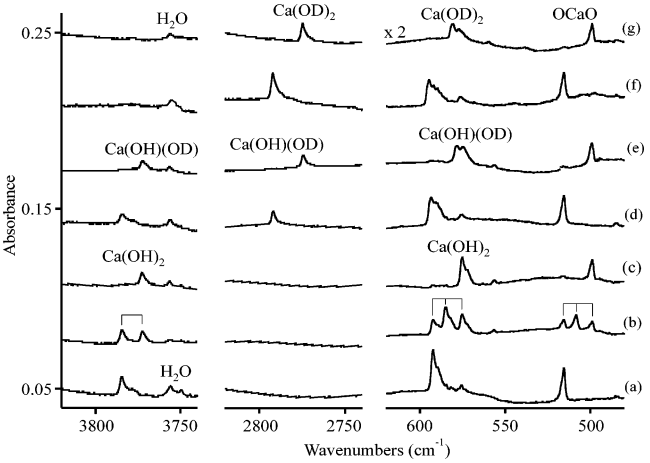

Figure 6. Infrared spectra in the 3820−3740, 2820−2740, and 620−480 cm^{-1} regions for ultraviolet photochemical reaction products of Ca atoms with 0.4% O_2 and 6% H_2 in solid argon at 10 K: (a) $^{16}O_2 + H_2$; (b) $^{16,18}O_2 + H_2$; (c) $^{18}O_2 + H_2$; (d) $^{16}O_2 + HD$; (e) $^{18}O_2 + HD$; (f) $^{16}O_2 + D_2$; (g) $^{18}O_2 + D_2$. Absorbance scale ×2 for the lowest region.

observed at 2788, 608.7 cm^{-1}: annealing decreased these bands and increased the 2746 and 577.6 cm^{-1} bands. The H_2 and $^{18}O_2$ reagents gave new absorptions at 3771, 589.2 cm^{-1}: annealing decreased these bands in favor of 3719 and 570 cm^{-1} absorptions. Finally, D_2 and $^{18}O_2$ produced new 2882 and 596.4 cm^{-1} absorptions, and annealing decreased these and produced broader 2734 and 558 cm^{-1} bands. The lower frequency region is illustrated in Figure 7.

Complementary experiments in pure hydrogen or deuterium with 0.1% O_2 gave sharp, split bands in the upper region and a broader band in the lower region, as listed in Table 2. The lower band yielded a partially resolved triplet absorption with $^{16,18}O_2$ in hydrogen and a broad doublet with $^{18}O_2$ in deuterium, as shown in Figure 7.

Sr. The reaction of laser-ablated Sr and O_2/H_2 in excess argon gave SrH_2 at 1134.2 cm^{-1}, weak SrO at 652.7 cm^{-1}, OSrO at 532.5 cm^{-1}, $(SrO)_2$ at 530.1, 441.5 cm^{-1}, and SrO_2 at 509.2 cm^{-1}, as observed with each reagent separately.[26,28] Weak new absorptions were also observed at 3760.6 and 479.0 cm^{-1}: these absorptions increased 3-fold upon $\lambda > 350$ nm irradiation, whereas the hydride and oxide products increased 2-fold or less. Continued irradiation at $\lambda > 290$ nm further increased the OSrO band and the 3760.6, 479.0 cm^{-1} pair, and raised very weak 498 cm^{-1} absorption above the noise level (Figure 2). A final 240−380 nm irradiation increased the 3760.6, 479.0 cm^{-1} pair by 30% with little effect on OSrO but destroyed SrH_2 absorptions.

Figure 8 illustrates the spectra with isotopic substitution in the reagents after 240−380 nm irradiation to maximize the new product absorptions. With a $^{16}O_2 + ^{18}O_2$ mixture and H_2, the upper band forms a 3760.6−3748.9 cm^{-1} doublet around the 3756 cm^{-1} water band and the lower band gives a 479.0−460.3 cm^{-1} doublet, as listed in Table 3. Using the $^{16}O_2 + ^{16}O^{18}O + ^{18}O_2$ mixture and H_2 gave the same upper doublet within experimental measurement error, but the lower doublet was broader and slightly shifted. The D_2 reagent shifted both bands, to 2773.6 and 470.6 cm^{-1}, and HD gave almost the same features as H_2 and D_2 with two bands in each region.

An experiment with Sr and H_2O_2 gave weak SrO_2, SrO, and OSrO bands, and the above new product absorptions at 3760.7 and 479.1 cm^{-1}. Irradiation at 240−380 nm increased the OSrO and latter absorptions by 30% and decreased the SrO and SrO_2 bands, and further irradiation at $\lambda > 220$ nm continued this effect. The 3760.7 and 479.1 cm^{-1} bands attained the intensities of the product bands in Figure 8a.

Parallel investigations with 3%H_2, 0.2% O_2 or 4% D_2 and 0.3% O_2 in excess neon gave the broader bands at 3749.8, 465 cm^{-1} or 2766.6, 454 cm^{-1} that are footnoted in Table 3. Using pure H_2 or D_2 with 0.2% O_2 gave sharper bands for the upper mode and broader bands for the lower mode, as found with calcium. Figure 9 compares spectra for the Sr reaction in the three matrix systems.

Ba. Laser-ablated Ba and O_2/H_2 samples also gave barium hydrides and oxides[26,28] and weak new absorptions, now shifted to 3724.2 and 422.8 cm^{-1}, as shown in Figure 10. The weak 459.0 cm^{-1} band is in agreement with the earlier assignment to HBaOH:[2] Here, it increases upon irradiation at 456.8 cm^{-1}. The former bands increase upon $\lambda > 380$ and 290 nm irradiations. However, 240−380 nm photolysis destroys BaH_2 and BaO_2, decreases BaO and $(BaO)_2$, slightly increases OBaO, and doubles the 3724.2 and 422.4 cm^{-1} absorptions with little effect at 456.8 cm^{-1}. A complementary experiment with Ba and H_2O_2 gave weak BaO, OBaO, $(BaO)_2$, and BaO_2 absorptions and a weak 423.0 cm^{-1} band. Unfortunately, the 3724 cm^{-1} region is masked by 3733 and 3725 cm^{-1} H_2O_2 photolysis product absorptions.[30b] Irradiation at 240−380 nm increased the oxide bands and the 423.0 cm^{-1} absorption and produced a weak 457.0 cm^{-1} band, as also shown in Figure 10.

Isotopic substitution again produced important diagnostic information. With the $^{18}O_2$ reagent and H_2, the new bands shifted to 3712.6 cm^{-1} and to a 404 cm^{-1} shoulder on the edge of our detection limit. However, $^{16,18}O_2$ produced a 3724−3712 cm^{-1} doublet, weak 422, 414 cm^{-1} bands, and a 457−435 cm^{-1} doublet. With $^{16}O_2$ and D_2, the bands shifted to 2746.6, 447.0, and 414.4 cm^{-1}, and the HD reagent gave two bands for the former two absorptions and a single intermediate band at 417.4 cm^{-1} for the latter absorption (Table 4). Irradiation ($\lambda > 220$ nm) also produced $H_2{}^{18}O$ at 3741 and 1586 cm^{-1} and D_2O at 1178 cm^{-1}.

TABLE 2: Infrared Absorptions (cm^{-1}) Produced upon Ultraviolet Irradiation of $Ca/O_2/H_2$ Samples in Solid Argon and Hydrogen

$^{16}O_2$, H_2	$^{16,18}O_2 + H_2$	$^{18}O_2 + H_2$	$^{16}O_2 + HD$	$^{18}O_2 + HD$	$^{16}O_2 + D_2$	$^{18}O_2 + D_2$
3784.6[a]	3784.3, 3772.3	3772.4[b]	3784.4, 2791.8	3772.3, 2774.4	2792.0[c]	2774.6[d]
592.4	592.4, 585.1, 575.3	575.3	593.6	578.6	594.8	581.0
575.7[e]	−, 556.6	556.6	575.7	556.4	576.4	559.8
3776.1[f]		3763.8[f]			2785.8[g]	2768.4[g]
3771.3		3759.2			2781.9	2764.5
578.2	578, 572, 364	563.5			581.7	572, 559

[a] Neon matrix counterpart at 3782 and 606.7 cm^{-1}. [b] Neon matrix counterpart at 3771 and 589.2 cm^{-1}. [c] Neon matrix counterpart at 2788 and 608.7 cm^{-1}. [d] Neon matrix counterpart at 2772 and 596.4 cm^{-1}. [e] Weak band is due to HCaOH based on agreement with ref 2: 1232.3 cm^{-1} absorption also observed but CaD_2 masked any 887 cm^{-1} DCaOD absorption. [f] In solid hydrogen. [g] In solid deuterium.

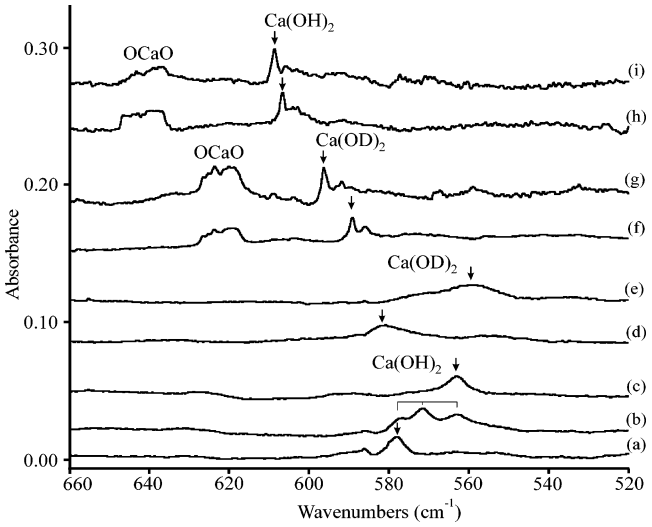

Figure 7. Infrared spectra in the 660−520 cm^{-1} region for ultraviolet photochemical reaction products of Ca, H_2, and O_2 in excess hydrogen, deuterium, or neon at 4 K: (a) $H_2 + {}^{16}O_2$; (b) $H_2 + {}^{16,18}O_2$; (c) $H_2 + {}^{18}O_2$; (d) $D_2 + {}^{16}O_2$; (e) $D_2 + {}^{18}O_2$; (f) $H_2 + {}^{18}O_2$ in neon; (g) $D_2 + {}^{18}O_2$ in neon; (h) $H_2 + {}^{16}O_2$ in neon; (i) $D_2 + {}^{16}O_2$ in neon. Sample concentrations: 0.1% O_2 in H_2 or D_2, and 3% H_2 and 0.2% in neon.

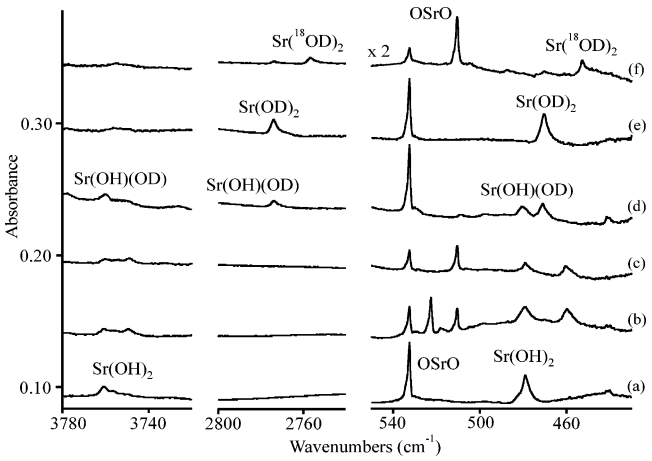

Figure 8. Infrared spectra in the 3780−3720, 2800−2740, and 550−430 cm^{-1} regions for the 240−380 nm photochemical reaction products of laser-ablated Sr atoms with 0.4% O_2 and 6% H_2 in solid argon at 10 K: (a) $^{16}O_2 + H_2$; (b)$^{16,18}O_2 + H_2$; (c) $^{16}O_2 + {}^{18}O_2 + H_2$; (d) $^{16}O_2 +$ HD; (e) $^{16}O_2 + D_2$; (f) $^{18}O_2 + D_2$. Absorbance scale ×2 for the lowest region.

Additional experiments with Ba and H_2/O_2 in neon gave a broader 3723 cm^{-1} band which shifted to 3712 cm^{-1} with $^{18}O_2$. In solid hydrogen, two bands were observed at 3718 and 410 cm^{-1} upon UV irradiation, and in solid D_2, the upper band shifted to 2742.2 cm^{-1} and the lower band was lost in the noise near 400 cm^{-1}.

The codeposition of laser-ablated Ba with D_2 containing 0.2% O_2 produced 2796.4 and 2745.6 cm^{-1} bands common to the D_2 system, plus weak bands at 727 cm^{-1} due to BaD_2, at 761.5 and 459.3 cm^{-1} due to BaO_2, and at 562.0 due to OBaO in solid deuterium.[26,28] The $\lambda > 350$ nm irradiation destroyed the 2796.4 and 2745.6 cm^{-1} bands, increased BaD_2 at 727 cm^{-1} to its maximum yield, increased BaO_2 and OBaO, and produced a weak 2742.2 cm^{-1} product band (Figure 11). The next $\lambda >$ 290 nm irradiation decreased BaD_2, BaO_2 and increased OBaO and the 2742.2 cm^{-1} product. Irradiation at 240−380 nm virtually destroyed the former and increased the latter. Full arc irradiation ($\lambda > 220$ nm) for 5 min decreased OBaO and doubled the 2742.2 cm^{-1} absorption, and 10 more min almost destroyed OBaO and doubled again the latter product band. A similar investigation with $^{18}O_2$ in D_2 gave the same 727 cm^{-1} absorption, but the other bands shifted to 719.3, 536.6, 439.0, and 2725.4 cm^{-1} with the same photochemical behavior pattern.

Calculations. Electronic structure calculations have been done for the OMO, MOH, HMOH, and $M(OH)_2$ molecules to help assign the new observed infrared absorptions and understand the structure and bonding in this interesting series of molecules. The results of our calculations at the B3LYP and MP2 levels of theory using the large 6-311++G(3df,3pd) basis set and SDD pseudopotential for Sr and Ba are summarized in Tables 5−8. Computations for Ca, Sr, and Ba dihydroxides gave imaginary O−M−O bending frequencies if all angles and distances were allowed to vary. Since our calculations found linear molecules for CaOH and BaOH, in agreement with earlier works involving both theory and experiment,[7−20] we fixed the M−O−H (M = Ca, Sr, and Ba) bond angles at 180° and adjusted all $M(OH)_2$ bond lengths and the O−M−O angle under C_{2v} symmetry. All real frequencies were obtained, as given in Tables 5 and 6, and the $Sr(OH)_2$ and $Ba(OH)_2$ molecules are clearly bent at the metal center, in agreement with earlier HF computations, which found nearly linear M−O−H linkages.[6] Figure 12 compares the structures obtained for the group 2 dihydroxide molecules.

The primary new result is the frequency calculations for the $M(OH)_2$ molecules, and two vibrational modes, the antisymmetric O−H and O−M−O stretching modes, give strong, observable infrared absorptions. A secondary result is the interesting family trend in O−H stretching frequencies and the mixing of vibrational modes with the O−M−O coordinate.

Discussion

The new group 2 $M(OH)_2$ molecules will be identified from the effect of isotopic substitution of O_2 and H_2 reagents on the two strongest infrared absorptions and comparison to frequencies calculated by electronic structure theory.

$Mg(OH)_2$. Two new infrared absorptions at 3829.8 and 867.2 cm^{-1} from the Mg + O_2 + H_2 reaction track together upon photolysis and annealing, and the isotopic shifts identify O−H and O−Mg−O stretching modes. The same absorptions are observed in the Mg atom reaction with H_2O_2. The isotopic

TABLE 3: Infrared Absorptions (cm^{-1}) Produced upon Ultraviolet Irradiation of $Sr/O_2/H_2$ Samples in Solid Argon and Hydrogen

$^{16}O_2 + H_2$	$^{16,18}O_2 + H_2$	$^{16}O_2 + {}^{18}O_2 + H_2$	$^{16}O_2 + HD$	$^{16}O_2 + D_2$	$^{18}O_2 + D_2$
3760.6[a]	3760.8, 3749.2	3760.6, 3748.9[b]	3760.2, 2773.8	2773.6[c]	2756.6[d]
498[e]					
479.0	479.3, 459.9	479.0, 460.3	480.2, 471.0	470.6	452.8
3749.8[f]		3738.2[f]		2766.6[g]	2749.7[g]
465		448		454.1	437.8

[a] Neon matrix counterpart at 3752 and 471.5 cm^{-1}. [b] Neon matrix counterpart at 3740 and 452.4 cm^{-1}. [c] Neon matrix counterpart at 2765.1 and 456.0. [d] Neon matrix counterpart at 2748.3 and 440.9 cm^{-1}. [e] Weak band is due to HSrOH.[2] [f] In solid hydrogen. [g] In solid deuterium.

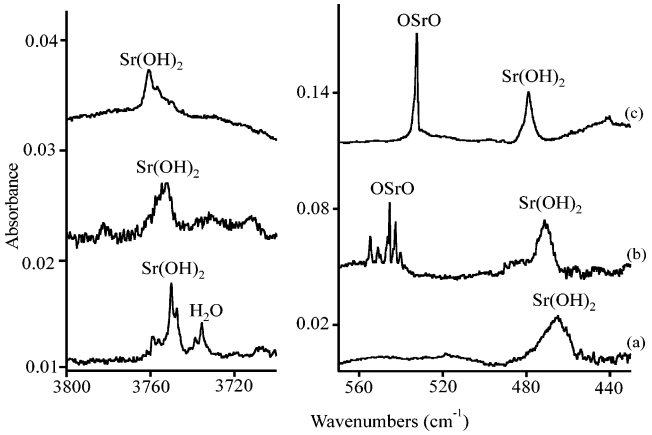

Figure 9. Infrared spectra in the 3800−3700 and 570−430 cm^{-1} regions for laser-ablated Sr codeposited with H_2 and O_2 and after 240−380 nm irradiation. (a) hydrogen matrix at 4 K; (b) neon matrix at 4 K; (c) argon matrix at 8 K.

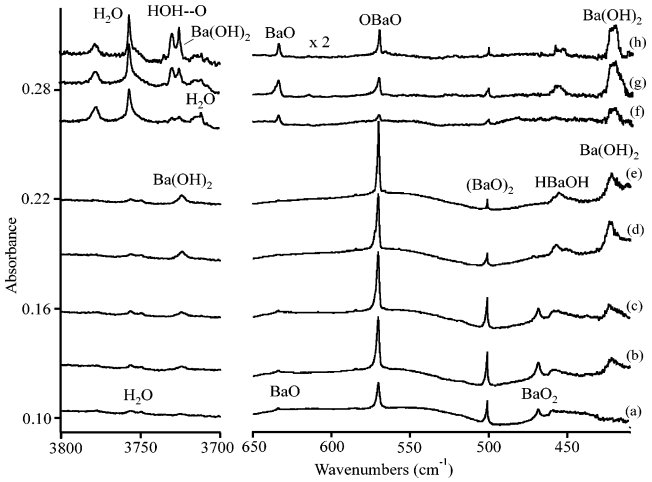

Figure 10. Infrared spectra in the 3780−3700 and 650−410 cm^{-1} regions for Ba atoms with 0.4% O_2 and 6% H_2 argon samples at 10 K: (a) laser-ablated Ba deposited with O_2 and H_2 in excess argon for 60 min, (b) after $\lambda > 350$ nm irradiation, (c) after $\lambda > 290$ nm irradiation, (d) after 240−380 nm irradiation, and (e) after annealing to 20 K. (f) laser-ablated Ba and H_2O_2 deposited in excess argon for 30 min, (g) after 240−380 nm irradiation for 30 min, and (h) after $\lambda > 220$ nm irradiation for 15 min.

frequency patterns obtained for the 867.2 cm^{-1} band show that a single Mg atom is involved from the natural magnesium-24,-25,26 intensities, which is like that observed for the analogous 767.7 cm^{-1} band of OMgO.[25] The oxygen isotopic triplet with $^{16}O_2$, $^{16}O^{18}O$, $^{18}O_2$ demonstrates that two equivalent oxygen atoms are included, and the 16/18 and 24/26 isotopic frequency ratios (1.02024, 1.02144) compare favorably to those observed for linear OMgO (1.02428, 1.02237) itself. Such information suggests a linear OMgO linkage in this new molecule. The observation of one HD component at 861.6 cm^{-1}, intermediate between the 867.2 and 854.8 cm^{-1} H_2 and D_2 values, indicates

TABLE 4: New Infrared Absorptions (cm^{-1}) Produced upon Ultraviolet Irradiation of $Ba/O_2/H_2$ Samples in Excess Argon

$^{16}O_2 + H_2$	$^{16,18}O_2 + H_2$	$^{18}O_2 + H_2$	$^{16}O_2 + HD$	$^{16}O_2 + D_2$
3724.2[a]	3724, 3712	3712.6[b]	3724.7, 2746.6	2746.6[c]
456.8[d]	457, 435	434.8	453.0, 446.4	447.0
422.8	422.8, 413, 403 sh	403 sh	417.4	414.4

[a] Neon matrix counterpart at 3723 cm^{-1}, solid hydrogen matrix at 3718 and 410 cm^{-1}. [b] Neon matrix counterpart at 3712 cm^{-1}. [c] Solid deuterium matrix at 2742.2 with ^{18}O counterpart at 2725.4 cm^{-1}. [d] Weak band is due to HBaOH based on agreement with ref 2: the 1059 cm^{-1} band is masked by BaH_2.

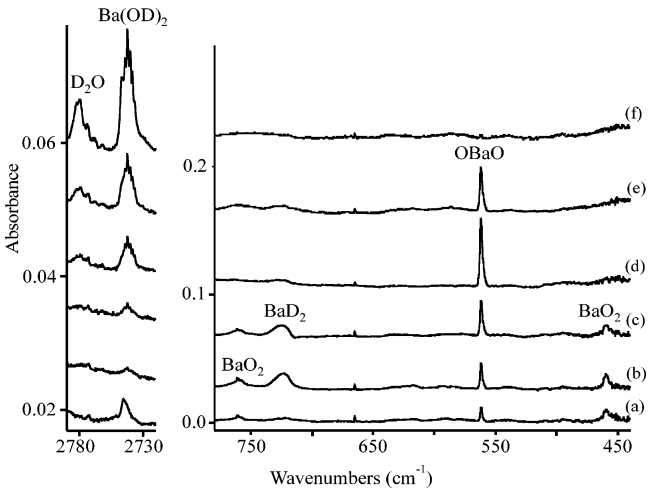

Figure 11. Infrared spectra in the 2790−2720 and 780−440 cm^{-1} regions for Ba codeposited at 4 K with D_2 containing 0.2% O_2: (a) laser-ablated Ba deposited, (b) after $\lambda > 350$ nm irradiation, (c) after $\lambda > 290$ nm irradiation, (d) after 240−380 nm irradiation, (e) after $\lambda > 220$ nm irradiation for 5 min, and (f) after $\lambda > 220$ nm irradiation for 10 min additional.

that two H(D) atoms are weakly coupled to the OMgO stretching mode, which is the same conclusion reached in our first identification of this absorption.[25] The new 3829.8 cm^{-1} absorption shifts appropriately for an O−H stretching mode (H/D ratio 1.3554, 16/18 ratio 1.00317). Unfortunately, coupling between the two equivalent O−H groups is so little that only an isotopic doublet is observed with $^{16}O_2$, $^{16}O^{18}O$, $^{18}O_2$, and the two bands observed with HD are the same as these found with H_2 and D_2. Hence, the new molecule has two O−H(O−D) groups, and these are equivalent based on the equivalent O atoms in the antisymmetric O−Mg−O stretching mode. Therefore, the $Mg(OH)_2$ molecule is identified through isotopic substitution at all atomic positions.

This identification of $Mg(OH)_2$ through two vibrational frequencies is confirmed by comparison with frequencies from our B3LYP and MP2 calculations. The calculations agree on the linear O−Mg−O linkage and predict the antisymmetric O−Mg−O stretching mode at 905.7 and 905.4 cm^{-1} (B3LYP and MP2, Tables 5 and 6), in excellent agreement with the 867.2 cm^{-1} observed value. Comparison of the calculated 16/18 and 24/26 harmonic isotopic frequency ratios also provides structural

TABLE 5: Frequencies, Bond Lengths, and Mulliken Charges Calculated on the Metal Center for HOMOH Molecules Converged at the B3LYP Level

metal	M−O, O−H[a] (Å)	O−M−O	*q* (M)	frequencies (cm^{-1}) (infrared intensities (km/mol))[b]
Be	1.423, 0.952	176°	−0.27	3993(23), 3991(198), 1536(423), 747(1), 529(101), 522(335), 314(28), 310(65), 190(129)
Mg	1.772, 0.949	180°	+1.05	4032(1), 4032(157), 906(198), 610(1), 162(1), 153(29), 153(50), 118(224), 21(219)
Ca	2.038, 0.954[c]	170°	+1.56	3960(2), 3960(82), 619(397), 525(1), 439(0), 438(1), 432(282), 432(268), 41(41)
Sr	2.186, 0.955[c]	155°	+1.58	3941(43), 3941(3), 491(3), 491(312), 433(0), 424(268), 423(257), 420(4), 29(32)
Ba	2.302, 0.956[c]	127°	+1.51	3918(29), 3918(9), 470(30), 441(307), 393(292), 388(0), 366(272), 329(30), 91(17)

[a] $Be(OH)_2$ and $Mg(OH)_2$ have computed dihedral angles of 96.8 and 139.9°, respectively. [b] Symmetric or antisymmetric O−H, antisymmetric or symmetric O−M−O stretching, M−O−H and O−M−O bending modes, respectively. [c] M−O−H angle fixed at 180°.

TABLE 6: Frequencies, Bond Lengths, and Mulliken Charges Calculated on the Metal Center for HOMOH Molecules Converged at the MP2 Level

metal	M−O, O−H[a] (Å)	O−M−O	*q* (M)	frequencies (cm^{-1}) (infrared intensities (km/mol))[b]
Be	1.433, 0.951	175°	0.14	4039(25), 4037(214), 1518(413), 736(1), 513(94), 503(331), 301(25), 293(67), 184(138)
Mg	1.771, 0.946[c]	180°	1.29	4106(0), 4106(205), 907(231), 606(0), 109(283 × 2), 52(0 × 2), 170(0 × 2)[d]
Ca	2.046, 0.953[c]	180°	1.72	4010(71), 4009(0), 626(374), 521(0), 457(270 × 2), 456(0 × 2), 47(50 × 2)
Sr	2.190, 0.954[c]	156°	1.75	3992(48), 3992(3), 499(248), 495(22), 491(0), 482(252), 481(12), 475(241), 44(40)
Ba	2.306, 0.956[c]	130°	1.66	3963(34), 3963(9), 474(3), 446(345), 440(291), 438(0), 421(290), 394(13), 72(22)

[a] $Be(OH)_2$ has a computed dihedral angle of 97.5°. [b] Symmetric or antisymmetric O−H, antisymmetric or symmetric O−M−O stretching, M−O−H and O−M−O bending modes, respectively. [c] M−O−H angle fixed at 180°. [d] This π_u bending mode has zero calculated intensity, which is suspect.

TABLE 7: Frequencies and Bond Lengths Calculated (B3LYP) for the HMOH and MOH Molecules

molecule	H−M, M−O, O−H (Å)	H−Ca−O, Ca−O−H	frequencies (cm^{-1}) (intensities (km/mol))
HCaOH	2.055, 2.011, 0.954	154°, 174°	3950(44), 1262(390), 598(199), 435(204), 425(189), 123(412)
DCaOD			2878(44), 902(217), 585(177), 329(135), 321(126), 90(2125)
CaOH	−, 1.976, 0.954	−, 180°	3959(72), 619(107), 358(88 × 2)
CaOD			2885(59), 606(101), 268(53 × 2)
HSrOH	2.202, 2.146, 0.955	133°, 170°	3941(33), 1157(412), 517(201), 411(191), 387(162), 209(343)
HBaOH	2.336, 2.258, 0.956	117°, 166°	3916(38), 1089(657), 476(236), 380(203), 329(147), 248(280)
BaOH	−, 2.225, 0.956	−, 180°	3920(73), 495(101), 342(63 × 2)

TABLE 8: Frequencies and Structures Calculated for the OMO Molecules

level	molecule	M−O	O−M−O	*q* (M)	frequencies (cm^{-1}) (intensities (km/mol))
B3LYP	OBeO, $^3\Sigma_g^-$	1.434	180°	−0.31	1377(340), 734(0), 165(121 × 2)
	OMgO, $^3\Sigma_g^-$	1.866	180°	1.10	781(113), 525(0), 130(112 × 2)
	OCaO, $^3B_2$	2.133	145°	1.37	535(280), 480(21), 58(79)
	OSrO, $^3B_2$	2.269	130°	1.50	449(31), 439(207), 107(45)
	OBaO, $^3B_2$	2.232	129°	1.37	440(35), 405(101), 92(31)
MP2	OBeO, $^3\Sigma_g^-$	1.421	180°	−0.22	1589(48), 781(0), 134(311 × 2)
	OMgO, $^3\Sigma_g^-$	1.786	180°	1.51	830(238), 563(0), 159(122 × 2)
	OCaO, $^3\Sigma_g^-$	2.021	180°	1.76	596(360), 498(0), 35(55 × 2)
	OSrO, $^3B_2$	2.261	133°	1.67	437(189), 414(52), 77(70)
	OBaO, $^3B_2$	2.325	117°	1.53	669(69), 565(464), 98(20)

information. These ratios (1.02154 and 1.02304 for B3LYP and 1.02236 and 1.02328 for MP2) are in excellent agreement with the observed 16/18 and 24/26 ratios (1.02024 and 1.02144) allowing for anharmonicity in the observed frequency, but B3LYP ratios are closer to the observed value (1.02144) because B3LYP predicts a 155.6° Mg−O−H angle and different mode mixing than MP2 with a completely linear molecule. Furthermore, both calculations predict the unobserved symmetric O−Mg−O stretching mode ~300 cm^{-1} lower, which will result in little mode mixing in the H−^{16}O−Mg−^{18}O−H molecule and allow the mixed 16,18 mode to be near the average of the 16,-16 and 18,18 values, as is observed (858.6 cm^{-1} average, 858.9 cm^{-1} observed, Table 1) and predicted by both calculations. The slightly better agreement with the 16/18 ratio computed for the bent molecule suggests a slightly nonlinear H−OMgO−H hydrogen attachment at oxygen, as found for the more covalent HOBeOH molecule.[4,5] Finally, we find no absorption at 742.3 cm^{-1}, which is expected for HMgOH from the Mg atom reaction with water.[2]

The calculations predict symmetric and strong antisymmetric O−H stretching modes at 4032.1, 4031.8 cm^{-1} (B3LYP) and 4105.7, 4105.5 (MP2) cm^{-1}, and the computed antisymmetric mode is in agreement with the observed 3829.8 cm^{-1} value, allowing for expected shortcomings in the computational methods (the calculated values are 5−7% too high).[34] Both calculations reveal almost identical O−H stretching modes, which shows that there is almost no coupling between them. This arises because these modes are essentially H atom vibrations and their coupling through the more massive O−Mg−O framework is limited. The calculated harmonic H/D and 16/18 frequency ratios, 1.3710 and 1.00346 (B3LYP), are higher than the observed values mostly because of anharmonicity.

$Ca(OH)_2$. The 3784.6 and 592.4 cm^{-1} absorptions from Ca + O_2 + H_2 track together upon irradiation and annealing in the Ca system. A 591.9 cm^{-1} absorption formed by the photochemical reaction of Ca and H_2O molecules was assigned by Kauffman et al.[2] to $Ca(OH)_2$. The key observation was a triplet absorption with mixed $H_2{}^{16}O$, $H_2{}^{18}O$, which indicated two equivalent oxygen atoms. Our observations of a similar 592.4 cm^{-1} absorption and the associated 3784.6 cm^{-1} O−H stretching mode with $Ca/O_2/H_2$ and with Ca/H_2O_2 support their assignment. Our isotopic frequencies are more accurate, owing to pure isotopic substitution using O_2 and H_2 without exchange and dilution from contaminants. The 16/18 ratio we observe for the strong 592.4 cm^{-1} band, 1.02972, is slightly lower than that determined for the bent triplet state OCaO molecule mode at 515.6 cm^{-1}.[26] This 16/18 ratio and the three-band pattern found

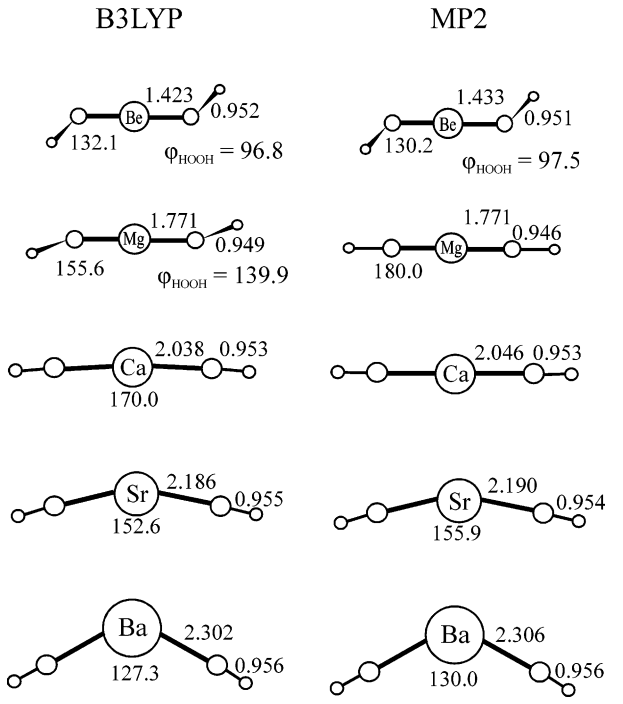

Figure 12. Structures calculated for $M(OH)_2$ molecules. The bond distances are in angstroms, and the bond angles are in degrees.

with $^{16}O_2 + {}^{16}O^{18}O + {}^{18}O_2$ strongly suggest that we are dealing with a new molecule containing two equivalent O atoms in a linear or nearly linear O−Ca−O linkage. As with $Mg(OH)_2$, two observations using HD are important: one new O−Ca−O stretching absorption that is intermediate between the H_2 and D_2 values, for both the $^{16}O_2$ and $^{18}O_2$ reactions, and separate O−H and O−D stretching modes indicate that two O−H(O−D) groups are involved in this molecule. Hence, $Ca(OH)_2$ is identified from detailed isotopic substitution in two diagnostic fundamental vibrational modes.

Our harmonic isotopic frequency calculations predict a 10 cm^{-1} red deuterium shift for the 592.4 cm^{-1} band and an 8 cm^{-1} red deuterium shift for the 576.3 cm^{-1} $^{18}O_2$ counterpart. Instead, 2.4 and 5.7 cm^{-1} blue shifts are observed for these modes, whereas 8−12 cm^{-1} red shifts are observed for the Mg, Sr, and Ba counterparts. Kauffman et al.[2] noted small blue deuterium shifts for their 591.9 cm^{-1} product absorption and the HCaOH band at 574.8 cm^{-1} and suggested a Fermi resonance interaction with the CaOH bending mode overtone. In fact, the Fermi resonance interaction that causes the blue deuterium shift in the O−Ca−O stretching mode is with the Ca−O−D bending mode combination band, as examination of our results for four pure isotopic frequencies in Table 2 clearly demonstrates. As stated above, the blue deuterium shift is larger (5.7 cm^{-1}) for the $^{18}O_2$ product than the $^{16}O_2$ product (2.4 cm^{-1}). This means that the perturbing level is closer to 575.3 cm^{-1} for $Ca(^{18}OD)_2$ than to 592.4 cm^{-1} for $Ca(^{16}OD)_2$. For example, let us estimate the combination band for $Ca(^{18}OD)_2$ as 574 cm^{-1}, and since our calculations find a 5 cm^{-1} ^{18}O shift in the fundamental, the combination band for $Ca(^{16}OD)_2$ would be at 584 cm^{-1}. Taking anharmonicity for CaOD bending from Jarman and Bernath[14] allows us to predict the bending fundamental for $Ca(^{16}OD)_2$ at 299 cm^{-1} and the combination at 584 cm^{-1} (294 and 574 cm^{-1} values for $Ca(^{18}OD)_2$). This 299 cm^{-1} bending fundamental estimate may be compared with the CaOD gas phase value of 266.8 cm^{-1}.[16] We note that the analogous Fermi resonance is weaker for CaOD, since the overtone of the bending mode falls short of the Ca−OD fundamental (near 604 cm^{-1}).[14,16] Finally, the CaOH/CaOD gas phase frequency ratio predicts a 389 cm^{-1} bending mode for $Ca(OH)_2$.

Our electronic structure calculations (Tables 5 and 6) for $Ca(OH)_2$ predict a nearly linear or linear molecule, in agreement with recent large basis set MP2 computations.[5] The important vibrational modes have nearly the same frequencies with both methods; for example the antisymmetric O−H and O−Ca−O stretching modes are 4010, 626 cm^{-1} (MP2) and 3960, 619 cm^{-1} (B3LYP). The agreement of these two computed frequencies (4−5% too high)[34] and their isotopic counterparts with our observed 3784.6, 592.4 cm^{-1} frequencies and isotopic data confirms our matrix identification of $Ca(OH)_2$ and the previous assignment of the O−Ca−O stretching mode.[2] Notice that our calculations predict a 78 or 95 cm^{-1} decrease in O−H stretching from $Mg(OH)_2$ to $Ca(OH)_2$ and we observe a 45 cm^{-1} decrease. Our calculations for $Ca(^{16}OH)(^{16}OD)$ and $Ca(^{18}OH)(^{18}OD)$ predict one strong O−Ca−O stretching mode intermediate between the all-H and all-D values and one such mode is observed. This and the observation of O−H and O−D stretching modes for the latter isotopic molecules clearly demonstrates that two O−H(O−D) groups are involved in this product molecule. Our calculations show that one intermediate mode is expected for $Ca(^{16}OH)(^{18}OH)$ at 7.7/17.7 of the way down from $Ca(^{16}OH)_2$ to $Ca(^{18}OH)_2$, and that is precisely what we observe (Table 3).

The experimental bending fundamental we predict at 389 cm^{-1} for $Ca(OH)_2$ from the Fermi resonance interaction in $Ca(OD)_2$ is in accord with both calculations of π_u and π_g bending modes in the 440−460 cm^{-1} region for the linear molecule and is higher than observed (near 350 cm^{-1})[14−16] for CaOH. The first overtone level of each bending mode has a σ_g component, which will not interact with the σ_u O−Ca−O stretching mode.[35] However, the $\pi_u + \pi_g$ combination band has an infrared active σ_u component, which can interact with the σ_u O−Ca−O stretching mode in Fermi resonance. Hence, the blue deuterium shifts observed for the σ_u modes of $Ca(^{16}OH)_2$ and $Ca(^{18}OH)_2$ are due to Fermi resonance with the combination of π_u and π_g bending modes.

Our B3LYP calculation predicts the Ca−O stretching mode in HCaOH to be 17.4 cm^{-1} lower than the strong O−Ca−O stretching mode for $Ca(OH)_2$, and the Virginia and Rice groups find it to be 16.7 or 17.1 cm^{-1} lower. Unfortunately, the O−H stretching mode is computed to be only 20% as strong and shifted only 4.3 cm^{-1} below that for $Ca(OH)_2$, and this mode cannot be observed.

The neon matrix effect on $Ca(OH)_2$ is to red shift the O−H stretching mode 2 cm^{-1} and blue shift the O−Ca−O mode 14 cm^{-1}, and the latter is much closer to the computed value. The positive deuterium shifts in the O−Ca−O mode for ^{16}O and ^{18}O are 2.0 and 7.2 cm^{-1}, which differ slightly from the 2.4 and 5.7 cm^{-1} values observed in solid argon. However, the hydrogen matrix red shifts the O−H mode even more (8 cm^{-1}) and also red shifts the O−Ca−O mode 14 cm^{-1}. The Fermi resonance interaction still operates in solid H_2/D_2, as seen by the positive deuterium shifts and the observation of both Fermi doublet components for $Ca(^{18}OD)_2$ in solid D_2 (Figure 7).

The red shifts in both $Ca(OH)_2$ fundamentals from solid argon to solid H_2/D_2 are reminiscent of the spectra of CaH_2, which is probably a slightly bent molecule and forms $(H_2)_nCaH_2$ complexes in solid H_2 with a 20 cm^{-1} red shift in the antisymmetric H−Ca−H stretching mode.[28] We believe that analogous $(H_2)_n$-$Ca(OH)_2$ complexes formed here are responsible for the red shifts from the argon matrix band positions. We expect the neon matrix to allow the formation of such complexes as well. The

more rigid argon matrix is formed faster, traps excess H_2, and retards the formation of such complexes. We expect $Ca(OH)_2$ to be essentially linear in the gas phase and the neon and argon matrix frequencies to be a good model for the gas phase values.

$Sr(OH)_2$. Two new absorptions at 3760.6 and 479.0 cm^{-1} increased together upon UV irradiation of the Sr, O_2, H_2 and Sr, H_2O_2, argon matrix samples. The 3760.6 cm^{-1} absorption behaved just like the Mg and Ca counterparts upon isotopic substitution, but the 479.0 cm^{-1} band exhibited different mode mixing. Our calculations for $Sr(OH)_2$ find a C_{2v} molecule, and the weak symmetric O−Sr−O stretching mode falls near the strong antisymmetric O−Sr−O stretching mode. However, in the lower symmetry $Sr(^{16}OH)(^{18}OH)$ molecule, both modes are of the same symmetry, and they are close enough to share intensity, but the higher mode is stronger. Our B3LYP calculation predicts these two modes for the latter mixed isotopic molecule 0 and 2 cm^{-1} below the strong modes for $Sr(^{16}OH)_2$ and $Sr(^{18}OH)_2$, so a broadened doublet is expected in the $^{16,18}O_2$ experiment, as is observed. In like fashion, the antisymmetric and symmetric O−Sr−O stretching modes share intensity in the HO−Sr−OD molecule, and the two modes are predicted 0 and 2 cm^{-1} below the all-H and all-D counterparts separated by 13 cm^{-1}. These bands are in fact closer (9.2 cm^{-1} apart) and more nearly equal in intensity than computed: two absorptions are observed at 480.2 and 471.0 cm^{-1}, near the H_2 and D_2 counterparts. Finally, our B3LYP calculations predict the b_2 O−H stretching mode of $Sr(OH)_2$ to be 19 cm^{-1} lower than that for $Ca(OH)_2$, and we observe it 24.0 cm^{-1} lower.

The strongest absorption observed in the Sr/H_2O system[2] at 498.2 cm^{-1} was identified as HSrOH: this band is barely detected in our experiment. The second strongest band at 479.3 cm^{-1}, first assigned to the SrOH molecule on the basis of straightforward isotopic behavior,[2] which we have shown above is not the case, must now be reassigned to $Sr(OH)_2$. Finally, our B3LYP calculation locates the Sr−O stretching mode in HSrOH to be 26 cm^{-1} above this mode for $Sr(OH)_2$, and we observe it 19 cm^{-1} higher.

The neon matrix effect on $Sr(OH)_2$ is to red shift the O−H stretching mode 9 cm^{-1} and the O−Sr−O mode 8 cm^{-1} from the argon matrix band positions and the ^{18}O shift is within 0.3 cm^{-1} for the O−H mode and 0.6 cm^{-1} less for the O−Sr−O mode. In addition, the neon matrix red shifts the analogous $Sr(OD)_2$ modes 8 and 14 cm^{-1}, and the ^{18}O shift is within 0.3 cm^{-1} for the O−D mode but 2.7 cm^{-1} smaller for the O−Sr−O mode than in solid argon. In solid hydrogen, the red shifts extend to 13 and 14 cm^{-1}, respectively, and the ^{18}O shift is within 0.1 cm^{-1} for the O−H mode and 2.7 for the O−Sr−O mode. In solid deuterium, the red shifts are 7 and 16 cm^{-1}, and the ^{18}O shift is within 0.1 cm^{-1} for the O−D mode but 1.5 cm^{-1} smaller for the O−Sr−O mode. Since solid hydrogen normally blue shifts from solid argon and solid neon blue shifts more from solid argon frequency positions, we interpret these shifts to indicate that $(H_2)_nSr(OH)_2$ complexes are forming in the lighter matrix hosts. The complex red shifts the bands with little effect on the normal modes as determined by isotopic shifts. We must also consider the possibility of a structural change. Our calculation for $Sr(OH)_2$ converged at an O−Sr−O angle of 152.6°. Fixing this angle at 162.6° decreased the O−H and O−Sr−O frequencies 1.1 and 0.5 cm^{-1}, and fixing this angle at 180° decreased the frequencies a total of 5.3 and 5.9 cm^{-1}, far less than the shift observed here from argon to neon to hydrogen. Although we expect argon to interact more strongly with the bent $Sr(OH)_2$ molecule than neon and hydrogen, and the O−Sr−O angle may well be a few degrees smaller in the more polarizable host, the 7−16 cm^{-1} matrix shifts observed here cannot be explained by structural change. These shifts are due to the formation of $(H_2)_nSr(OH)_2$ complexes, and similar shifts were found for the analogous $(H_2)_nSrH_2$ complexes.[28]

$Ba(OH)_2$. The barium, oxygen, hydrogen system followed these trends and produced two new absorptions at 3724.2 and 422.8 cm^{-1} with appropriate isotopic behavior for $Ba(OH)_2$. These bands shifted to 2746.6 and 414.4 cm^{-1} with D_2, but with the HD reagent, 3724.2 and 2746.6 cm^{-1} absorptions were observed in the upper region and a single intermediate 417.4 cm^{-1} band was observed in the lower region. For the latter b_2 O−Ba−O stretching mode, our calculations find a 12 cm^{-1} red shift for $Ba(OD)_2$ and a 7 cm^{-1} red shift for Ba(OH)(OD) and we observe 8.4 and 5.4 cm^{-1} red shifts. Furthermore, our MP2 calculation predicts the symmetric O−Ba−O stretching mode in HO−Ba−OH to be 28 cm^{-1} higher than the antisymmetric mode and only one of the HO−Ba−OD stretching modes to have observable intensity. With $^{18}O_2$, the 3724.2 cm^{-1} band shifts to 3712.6 cm^{-1} and the 422.8 cm^{-1} band results in a 404 cm^{-1} shoulder on the detection limit of our instrument. With $^{16,18}O_2$, a 3724.2−3712.6 cm^{-1} doublet is observed in the upper region and the lower region reveals weak 423 and 413 cm^{-1} bands on the detection limit. On the basis of the trends in observed and calculated frequencies for $Mg(OH)_2$, $Ca(OH)_2$, and $Sr(OH)_2$, we assign the 3724.2 and 422.8 cm^{-1} bands to $Ba(OH)_2$. Our B3LYP calculation predicts a 50 cm^{-1} red shift from the Sr to the Ba species, and we observe a 36.4 cm^{-1} shift in solid argon. Finally, we observed a 50% stronger absorption at 423.0 cm^{-1} for the Ba and H_2O_2 reaction to form $Ba(OH)_2$, but the 3724 cm^{-1} band was masked.

Calculations were done for HOBaOH with the O−BaO angle fixed at 128.4° (value for $BaCl_2$), 138.4 and 148.4° and Ba−O−H fixed at 180°. The important frequencies decreased from 3918, 440 cm^{-1} to 3913, 432 cm^{-1} to 3908, 424 cm^{-1}, and only in the latter case was the lowest frequency imaginary. The O−Ba−O angle was optimized to 127.4°, and the frequencies 3918 and 441 cm^{-1} were obtained.

The small frequency decreases in neon and in solid H_2 or D_2 are attributed to the formation of $(H_2)_nBa(OH)_2$ complexes, as found for $(H_2)_nBaH_2$.[28] Smaller such shifts were observed for the larger $Ba(OH)_2$ molecule, suggesting a weaker interaction with dihydrogen. Hence, the 7 cm^{-1} decrease from argon to hydrogen is more likely due to complex formation than valence angle increase.

Kauffman et al. observed four bands in the lower frequency region.[2] The strongest band at 458.9 cm^{-1} was assigned to HBaOH, and our weak 456.8 cm^{-1} absorption is probably due to this same molecule. A weak 430.1 cm^{-1} band, which we do not observe, was assigned to BaOH, but our calculations predict this mode much higher. Another weak band at 482.1 cm^{-1}, which we do not observe, was assigned to $Ba(OH)_2$. Unfortunately, the ^{18}O counterparts were not clear, owing to the lack of pure $H_2{}^{18}O$ substitution. A final weak band at 422.6 cm^{-1} was unassigned: this band is assigned here to $Ba(OH)_2$ as described above. Our B3LYP calculations find the Ba−O stretching mode for $Ba(OH)_2$ to be 35 cm^{-1} below this mode for HBaOH, and our assignment places this band 34 cm^{-1} lower.

Reaction Mechanisms. The stable $M(OH)_2$ molecules are prepared in major yield from the photoexcited metal atom reaction with O_2, H_2 mixtures. The wavelength selective irradiations determine that ^1P is the reactive metal atom state[36] in these experiments, as found recently for the corresponding reactions with H_2, although gas phase reactions with energetic laser-ablated metal atoms may involve the ^3P state.[28,37,38] The

triplet OMO molecules are all stable,[25,26] and we propose that the primary reaction proceeds through an excited OMO intermediate species to the metal dihydroxide molecules. The $M(OH)_2$ molecules are very stable, as expected: we compute $\Delta E = -235$, -174, -190, -185, and -198 kcal/mol for reaction 1 at the MP2 level (M = Be, Mg, Ca, Sr, and Ba, respectively). We form a minor amount of isotopically enriched water, so little decomposition of the stable isolated $M(OH)_2$ product appears to occur under the conditions of our argon matrix experiments. However, with neon or pure H_2, excess hydrogen is available and H_2O and $(H_2O)_2$ are also formed. We produce a very small yield of the HMOH molecules (none for Mg), and this probably arises from further reaction 2 of the MO molecule, which is a minor product of the laser-ablated metal atom reaction with O_2.[25,26] We note the absence of MgO and HMgOH in these experiments and the small yield of MO and HMOH (M = Ca, Sr, and Ba).

$$M + O_2 + H_2 \rightarrow [OMO^*] + H_2 \rightarrow HOMOH \quad (1)$$

$$M + O_2 + 2H_2 \rightarrow [MO^*] + O + 2H_2 \rightarrow HMOH + H_2O \quad (2)$$

$$M + O_2 + 2H_2 \rightarrow [OMO^*] + 2H_2 \rightarrow M + 2H_2O \quad (3)$$

Both MH_2 and MO_2 are photochemical reaction products as well, but their wavelength selective rise and fall behavior are different. This is clearly observed with Ba in pure D_2 where the oxide products are less stable (Figure 11). The initial $\lambda > 350$ nm irradiation forms considerable BaD_2, and a small amount of OBaO and $Ba(OD)_2$, and 240−380 nm photolysis destroys BaD_2 and increases the latter absorptions. The final $\lambda > 220$ nm irradiation cycles decrease and almost destroy OBaO and markedly increase $Ba(OD)_2$ at 2742.2 cm^{-1}. This shows that the reaction proceeds through the OBaO molecule intermediate, which activates D_2 to form $Ba(OD)_2$. Considerable D_2O and $(D_2O)_2$ are observed as well.

$$Ba + D_2 + O_2 \rightarrow OBaO + D_2 \rightarrow Ba(OD)_2 \quad (4)$$

The M atom insertion reaction with H_2O_2 is straightforward, and sharp $M(OH)_2$ product absorptions are observed in agreement with those from the $O_2 + H_2$ reagents. The weak OMO absorptions probably arise from reactions with O_2 from the decomposition of H_2O_2, and HCaOH is produced by the reaction with H_2O. Our observation of the same product absorptions with the H_2O_2 and $O_2 + H_2$ reagents confirms the present identification and assignments for the $M(OH)_2$ molecules. Reaction 5 is also highly exothermic but less so than reaction 1 by the energy of formation of H_2O_2 (−31 kcal/mol at the MP2 level). We observe slightly more CaO, SrO, and BaO using H_2O_2 than with $O_2 + H_2$, which likely arises from decomposition of the energized dihydroxide product of reaction 5.

$$M + H_2O_2 \rightarrow M(OH)_2 \quad (5)$$

Family Relationships. Several trends in group 2 metal dihydroxides and their chemistry merit attention. First the O−H stretching frequency in the alkaline earth metal dihydroxide molecules decreases from 3829.8 to 3784.6 to 3760.6 to 3724.2 cm^{-1} in solid argon for the Mg to Ba series, while the Mulliken charge computed on the metal center at the MP2 level increases from +1.29 to 1.72 to 1.75 and then falls to 1.66, although the computed Mulliken charge is likely an overestimate of the actual charge. The $M(OH)_2$ molecule frequencies approach but do not reach the solid state $Ca(OH)_2$ value (3644 cm^{-1}) or the gas phase OH^- value (3555.6 cm^{-1}).[39,40] Apparently some (cation)(anion) polarization and $p_\pi \rightarrow d_\pi$ interaction[6] reduce the degree of charge transfer in the isolated molecule. The Ca, Sr, and Ba dihydroxide molecules are predominately ionic with a small covalency that involves more d character going down the family group. The O−M−O angles we calculate here at the B3LYP and MP2 levels (Tables 5 and 6) are in excellent agreement with the HF values (180, 151, and 131°) of Kaupp and Schleyer,[6] who discuss how π-type bonding contributions prevent as much bending as that found for the difluorides.

On the other hand, the O−H stretching mode for $Be(OH)_2$ falls intermediate between the Mg and Ca dihydroxide values and the $Be(OH)_2$ molecule has substantial covalent character from the bent BeOH bond angles, the molecular dihedral angle,[4,5] and the much smaller Mulliken charge on the Be center (Tables 5 and 6). Clearly, $Mg(OH)_2$ shows the beginnings of ionic character. Our calculated structural parameters for the Be, Mg, and Ca dihydroxides agree with the large basis set values of the Radom group.[5] The O−Be−O stretching mode in the dihydroxide at 1493.7 cm^{-1} is above that for OBeO itself at 1413.2 cm^{-1}.[4]

Another difference with $Be(OH)_2$ is that the neon matrix blue shifts the argon matrix 3805.9 and 1493.7 cm^{-1} fundamentals[4] to higher 3833.6 and 1511.0 cm^{-1} frequencies observed here from beryllium reactions with O_2 and H_2 in excess neon, which is expected for the neon matrix. It follows then that $Be(OH)_2$ does not form complexes with H_2 to the extent of its heavier family members, a property also shared with BeH_2.

Barium appears to be the less reactive group 2 metal under the conditions of these experiments. The OBaO molecule was the only dioxide that survived in solid D_2 (Figures 4 and 11), but $\lambda > 220$ nm irradiation ultimately converts the dioxide to the dihydroxide. Note that OBaO red shifted in solid D_2 by 8 cm^{-1} from the argon matrix value (570.2 cm^{-1}),[26] and this suggests $(D_2)_n(OBaO)$ complex formation at the metal center.

Other comparisons can be made with the CaOH and CaOD molecules. The O−H and O−D stretching fundamentals for the latter molecules have been determined at 3778 and 2790 ± 3 cm^{-1} from gas phase emission spectra.[15] Our argon matrix O−H and O−D fundamentals for $Ca(OH)_2$ and $Ca(OD)_2$ are 3784.6 and 2792.0 cm^{-1}, respectively, and we predict gas phase positions near 3790 and 2800 cm^{-1} for the dihydroxide molecules. This close agreement is substantiated by our calculations, which gave virtually the same O−H bond lengths and frequencies for both molecules. Next, the Ca−O stretching fundamental for gaseous CaOH is near 609 cm^{-1}[1,14,16] and this is near our σ_u mode, which is higher than the computed σ_g mode by ~100 cm^{-1} for $Ca(OH)_2$. Our calculations suggest slightly stronger bonding in CaOH, as the Ca−O bond length is 0.05−0.06 Å shorter than that computed for $Ca(OH)_2$ by the two methods. Finally, the bending mode frequency deduced here for $Ca(OH)_2$ (389 cm^{-1}, π_u and π_g modes are nearly the same) is higher than that observed for CaOH (~350 cm^{-1}),[14−16] which is also in accord with our computations.

We note that the O−Ca−O stretching mode for $Ca(OH)_2$ shifts from 592.4 cm^{-1} in argon to 606.7 cm^{-1} in neon, which is the only blue shift observed for the heavy $M(OH)_2$ molecules, and the red shift on the O−H mode (2−3 cm^{-1}) is much less than that observed for $Sr(OH)_2$ (8−9 cm^{-1}). We conclude that $Ca(OH)_2$ is less extensively complexed by H_2 than $Sr(OH)_2$ in solid neon.

Another interesting trend is the antisymmetric O−M−O frequency in the isolated dioxide molecule and in the dihydroxide molecule. Figure 2 contrasts the smooth decrease in this

mode for the dihydroxides with the reversal at Ca for the dioxides. The OMgO molecule is linear,[27,41] OCaO is likely to be slightly bent (the calculated valence angle depends on the method employed),[26,42] and the OSrO and OBaO molecules are probably bent, although their matrix infrared observation reveals no structural information.[26] Our B3LYP and MP2 calculations find the latter molecules to be bent (Table 8, 133−117°), which are consistent with bent structures for the SrH_2, BaH_2, SrX_2, and BaX_2 (X = Cl and Br)[6,28,43] triatomic molecules, although the calculated frequency match for OSrO and OBaO is not as good as that for the dihydroxides. We include Mulliken charges on the metal center for the OMO molecules: Notice that OCaO is the most ionic of the dioxides (MP2 level), and this is where the frequency trend abruptly changes, suggesting an associated structure change. However, notice the gradual decrease in frequency and increase in Mulliken charge at the metal center for the dihydroxides, which have bent O−M−O linkages for $Sr(OH)_2$ and $Ba(OH)_2$. The slight decrease in charge at Ba compared to Sr is probably due to increased polarizability of the larger barium cation center compared to the smaller strontium cation. The same effect has been observed for SrO and BaO in the gas phase where SrO has the larger ionic character.[44,45] Finally, the ionic characters noted here for the strontium and barium monoxides, dioxides, and dihydroxides are all consistent.

Conclusions

Reactions of laser-ablated Mg, Ca, Sr, and Ba atoms with O_2, H_2 mixtures produce new absorptions in the O−H and O−M−O stretching regions, which increase together upon UV photolysis and are due to the $M(OH)_2$ molecules (M = Mg, Ca, Sr, and Ba). The $M(OH)_2$ identifications are supported by pure and mixed isotopic substitution, production of the same $M(OH)_2$ absorptions using H_2O_2 as the reagent, and theoretical calculations (B3LYP and MP2). The O−H stretching frequencies of the alkaline earth metal dihydroxide molecules decrease from 3829.8 to 3784.6 to 3760.6 to 3724.2 cm^{-1} in the family series in solid argon, while the base strength of the solid compounds increases. Although these molecules are predominantly ionic, the OH stretching frequencies do not reach the ionic limit of gaseous OH^- going down the family group because of cation−anion polarization and $p_\pi \rightarrow d_\pi$ interactions. The antisymmetric O−M−O stretching modes decrease from 867.2 to 592.4 to 479.0 to 422.8 cm^{-1} in the family series in solid argon. Calculations show that $Mg(OH)_2$ and $Ca(OH)_2$ are linear or nearly linear at the metal center but that $Sr(OH)_2$ and $Ba(OH)_2$ are bent at the metal center, owing to d orbital involvement in the bonding. Matrix shifts observed for these molecules in solid neon and hydrogen suggest the formation of $(H_2)_nM(OH)_2$ complexes.

Acknowledgment. We thank the N.S.F. for support by grant CHE 03-52487 and L. Khriachtchev for helpful suggestions on the use of urea−hydrogen peroxide.

References and Notes

(1) Cotton, F. A.; Wilkinson, G.; Murillo, C. A.; Bochmann, M. *Advanced Inorganic Chemistry*, 6th ed.; Wiley: New York, 1999.

(2) Kauffman, J. W.; Hauge, R. H.; Margrave, J. L. *High Temp. Sci.* **1984**, *18*, 97.

(3) Tague, T. J., Jr.; Andrews, L. *J. Phys. Chem.* **1994**, *98*, 8611.

(4) Thompson, C. A.; Andrews, L. *J. Phys. Chem.* **1996**, *100*, 12214.

(5) Schultz, A.; Smith, B. J.; Radom, L. *J. Phys. Chem. A* **1999**, *103*, 7522.

(6) Kaupp, M.; Schleyer, P. v. R. *J. Am. Chem. Soc.* **1992**, *114*, 491.

(7) Paeke, W. E.; Kirtman, B. *Chem. Phys. Lett.* **1985**, *117*, 424.

(8) Bauschlicher, C. W., Jr.; Langhoff, S. R.; Partridge, H. *J. Chem. Phys.* **1986**, *84*, 901.

(9) Koput, J.; Carter, S.; Peterson, K. A.; Theodorakopoulos, G. *J. Chem. Phys.* **2002**, *117*, 1529 and references therein.

(10) Koput, J.; Peterson, K. A. *J. Phys. Chem. A* **2003**, *107*, 3981 and references therein.

(11) Koput, J.; Peterson, K. A. *J. Phys. Chem. A* **2002**, *106*, 9595 and references therein.

(12) (a) Nakagawa, J.; Wormsbecher, R. F.; Harris, D. O. *J. Mol. Spectrosc.* **1983**, *97*, 37. (b) Hilborn, R. C.; Zhu, Q. S.; Harris, D. O. *J. Mol. Spectrosc.* **1983**, *97*, 73.

(13) (a) Ni, Y. Ph.D. Thesis, University of California, Santa Barbara, CA, 1986. (b) Bunker, P. R.; Kolbuszewski, M.; Jensen, P.; Brumm, M.; Anderson, M. A.; Berclay, W. L.; Ziurys, L. M.; Ni, Y.; Harris, D. O. *Chem. Phys. Lett.* **1995**, *239*, 217.

(14) Jarman, C. N.; Bernath, P. F. *J. Chem. Phys.* **1992**, *97*, 1711.

(15) (a) Pereira, R.; Levy, D. H. *J. Chem. Phys.* **1996**, *105*, 9733. (b) Levy, D. H. Personal communication, 2004.

(16) (a) Presunka, P. I.; Coxon, J. A. *J. Chem. Phys.* **1994**, *101*, 201. (b) Li, M.; Coxon, J. A. *J. Chem. Phys.* **1995**, *102*, 2663; **1996**, *104*, 4961 and references therein.

(17) Apponi, A. J.; Anderson, M. A.; Ziurys, L. M. *J. Chem. Phys.* **1999**, *111*, 10919.

(18) Beardah, M. S.; Ellis, A. M. *J. Mol. Spectrosc.* **2003**, *218*, 80 and references therein.

(19) Fernando, W. T. M. L.; Douay, M.; Bernath, P. F. *J. Mol. Spectrosc.* **1990**, *144*, 344 and references therein.

(20) Pooley, S. J.; Beardah, M. S.; Ellis, A. M. *J. Electron Spectrosc. Relat. Phenom.* **1998**, *97*, 77.

(21) Murad, E. *J. Chem. Phys.* **1981**, *75*, 4080.

(22) Andrews, L.; Wang, X. *Inorg. Chem.* **2005**, *44*, 11.

(23) (a) Andrews, L.; Citra, A. *Chem. Rev.* **2002**, *102*, 885 and references therein. (b) Andrews, L. *Chem. Soc. Rev.* **2004**, *33*, 123.

(24) Frisch, M. J.; Trucks, G. W.; Schlegel, H. B.; Scuseria, G. E.; Robb, M. A.; Cheeseman, J. R.; Zakrzewski, V. G.; Montgomery, J. A., Jr.; Stratmann, R. E.; Burant, J. C.; Dapprich, S.; Millam, J. M.; Daniels, A. D.; Kudin, K. N.; Strain, M. C.; Farkas, O.; Tomasi, J.; Barone, V.; Cossi, M.; Cammi, R.; Mennucci, B.; Pomelli, C.; Adamo, C.; Clifford, S.; Ochterski, J.; Petersson, G. A.; Ayala, P. Y.; Cui, Q.; Morokuma, K.; Malick, D. K.; Rabuck, A. D.; Raghavachari, K.; Foresman, J. B.; Cioslowski, J.; Ortiz, J. V.; Stefanov, B. B.; Liu, G.; Liashenko, A.; Piskorz, P.; Komaromi, I.; Gomperts, R.; Martin, R. L.; Fox, D. J.; Keith, T.; Al-Laham, M. A.; Peng, C. Y.; Nanayakkara, A.; Gonzalez, C.; Challacombe, M.; Gill, P. M. W.; Johnson, B.; Chen, W.; Wong, M. W.; Andres, J. L.; Gonzalez, C.; Head-Gordon, M.; Replogle, E. S.; Pople, J. A. *Gaussian 98*, revision A. 6; Gaussian, Inc.: Pittsburgh, PA, 1998 (and references therein).

(25) Andrews, L.; Yustein, J. T. *J. Phys. Chem.* **1993**, *97*, 12700.

(26) Andrews, L.; Yustein, J. T.; Thompson, C. T.; Hunt, R. D. *J. Phys. Chem.* **1994**, *98*, 6514.

(27) Wang, X.; Andrews, L. *J. Phys. Chem. A* **2004**, *108*, 11511.

(28) Wang, X.; Andrews, L. *J. Phys. Chem. A* **2004**, *108*, 11500 (Ca, Sr, Ba + H_2).

(29) (a) Milligan, D. E.; Jacox, M. E. *J. Chem. Phys.* **1963**, *38*, 2627. (b) Smith, D. W.; Andrews, L. *J. Chem. Phys.* **1974**, *60*, 81.

(30) (a) Pettersson, M.; Tuominen, S.; Rasanen, M. *J. Phys. Chem. A* **1997**, *101*, 1166. (b) Pehkonen, S.; Pettersson, M.; Lundell, J.; Khriachtchev, L.; Rasanen, M. *J. Phys. Chem. A* **1998**, *102*, 7643.

(31) A strong structured absorption appears at 3000−2700 cm^{-1} with Mg and O_2 and is destroyed upon irradiation. This absorption shifts with $^{18}O_2$ and is believed to be an electronic transition of a Mg_xO_2 cluster.

(32) Thompson, W. E.; Jacox, M. E. *J. Chem. Phys.* **1989**, *91*, 3826.

(33) (a) Redington, R. L.; Milligan, D. E. *J. Chem. Phys.* **1962**, *37*, 2162. (b) Ayers, G. P.; Pullin, A. D. E. *Spectrochim. Acta* **1976**, *32A*, 1629 and references therein.

(34) Scott, A. P.; Radom, L. *J. Phys. Chem.* **1996**, *100*, 16502.

(35) Wilson, E. B., Jr.; Decius, J. C.; Cross, P. C. *Molecular Vibrations*; McGraw-Hill, New York, 1955.

(36) Moore, C. E. *Atomic Energy Levels*, Nat. Bur. Stds, Circular 467, Washington, D.C., **1952**.

(37) Kang, H.; Beauchamp, J. L. *J. Phys. Chem.* **1985**, *89*, 3364.

(38) Bernath, P. F. *Advances in Photochemistry*; John Wiley: 1997; Vol. 23.

(39) Lagarde, P.; Nerenberg, M. A. H.; Farge, Y. *Phys. Rev. B* **1973**, *8*, 1731.

(40) Rosenbaum, N. H.; Owrutsky, J. C.; Tack, L. M.; Saykally, R. J. *J. Chem. Phys.* **1986**, *84*, 5308.

(41) Bauschlicher, C. W., Jr.; Langhoff, S. R.; Sodupe, M. *J. Phys. Chem.* **1992**, *96*, 9259.

(42) Andrews, L.; Chertihin, G. V.; Thompson, C. A.; Dillon, J.; Byrne, S.; Bauschlicher, C. W., Jr. *J. Phys. Chem.* **1996**, *100*, 10088.

(43) Hargittai, M. *Chem. Rev.* **2000**, *100*, 2233.

(44) Wharton, L.; Kaufman, M.; Klemperer, W. *J. Chem. Phys.* **1962**, *37*, 621.

(45) Kaufman, M.; Wharton, L.; Klemperer, W. *J. Chem. Phys.* **1965**, *43*, 943.